Initial tests on deghosting

Jingfeng Zhang and Arthur B. Weglein
University of Houston

Abstract

We present some initial tests on the deghosting algorithm given by Weglein et al. (2002). Given the pressure field on a towed streamer and the wavelet, the algorithm works very well. If the wavelet is not available, we present a way to approximate the wavelet using pressure measurements on a single towed streamer. Numerical tests show that, when using the approximated wavelet, the deghosting algorithm also works well. To the current state of testing, we are encouraged to continue further testing and analysis of the deghosting algorithm for towed streamer data. For ocean bottom pressure measurements and an estimate of the wavelet, we are reporting that early tests indiciate this method will be a stable method for deghosting without a geophone measurement, and is insensitive to the depth of the pressure measurement.

1 Introduction

Deghosting (up/down-going wave field separation) plays an important role in seismic data processing. In particular, it is a prerequisite for wave-theoretic free surface multiple removal algorithms (e.g., Weglein et al. 1997). In turn, the removal of free surface multiples, is a prerequisite for inverse scattering internal multiple attenuation, as well as most imaging algorithms and AVO analysis.

In this paper, we analyze the algorithm presented by Weglein et al. (2002) for the towed streamer case. The basic idea is to first use the data on the measurement surface (ms) to predict the wave field and its derivative on a pseudo-measurement surface ($\tilde{ms}$), then plug the predicted value into an integral which "generates" the deghosted data (or, up-going wave field) on a new surface. The $\tilde{ms}$ must be above the actual ms and then the deghosted data is then output at any point above $\tilde{ms}$.

For the case when the source is positioned between the measurement surface and the free surface, we have also tried to apply this deghosting algorithm without knowledge of the source wavelet.

Calculations, have shown that, without knowledge of the source wavelet, the wave field is well predicted, even directly under the source as long as $\tilde{ms}$ is close to the actual ms; the

predicted derivative of the wave field is good only for the positions with large offset. For positions directly under the source, the result for the derivative of the field is poor. In order to predict a good derivative of the wave field under the source, we provide a way to approximate the wavelet that relies on the assumption that a term containing the integral of the scattered field is relatively small compared to a similiar term containing the integral of the direct wave field $A(\omega)G_0^D(\mathbf{r}^{''},\mathbf{r}_s,\omega)$.

In the following, we briefly list the necessary formulae in the theory section and then present the results of numerical tests.

2 Theory

The deghosting formula is (Weglein et al., 2002):

$$P^{\text{deghosted}}(\mathbf{r},\mathbf{r}_s,\omega)=\int\limits_{ms}\left(P(\mathbf{r}^{'},\mathbf{r}_s,\omega)\frac{\partial G_0^+(\mathbf{r},\mathbf{r}^{'},\omega)}{\partial\mathbf{n}^{'}}-G_0^+(\mathbf{r},\mathbf{r}^{'},\omega)\frac{\partial P(\mathbf{r}^{'},\mathbf{r}_s,\omega)}{\partial\mathbf{n}^{'}}\right)d\mathbf{s}^{'} \qquad (1)$$

where G_0^+ is the causal Green's function in the reference medium. If we have the field and its derivative on the measurement surface, then the integral in equation (1) provides the deghosted field. However, in a conventional towed-streamer marine survey, we usually only measure the field, and not its normal derivative. In this research, we are investigating the effectiveness of equation (1) using data on the ms to predict the field and its derivative on a new pseudo measurement surface ($\tilde{ms}$). If successful, we can perform deghosting using equation (1) on $\tilde{ms}$.

The wavefield and its normal derivative predicted above the cable are (T.H. Tan, 1992 and 1999, A. Osen, 1998 and Weglein et al., 2002):

$$P(\mathbf{r}^{''},\mathbf{r}_s,\omega)=A(\omega)G_0^{DD}(\mathbf{r}^{''},\mathbf{r}_s,\omega)+\int\limits_{ms}P(\mathbf{r}^{'},\mathbf{r}_s,\omega)\frac{\partial G_0^{DD}(\mathbf{r}^{'},\mathbf{r}^{''},\omega)}{\partial\mathbf{n}^{'}}d\mathbf{s}^{'} \qquad (2)$$

$$\frac{\partial P(\mathbf{r}^{''},\mathbf{r}_s,\omega)}{\partial\mathbf{n}^{''}}=A(\omega)\frac{\partial G_0^{DD}(\mathbf{r}^{''},\mathbf{r}_s,\omega)}{\partial\mathbf{n}^{''}}+\int\limits_{ms}P(\mathbf{r}^{'},\mathbf{r}_s,\omega)\frac{\partial^2 G_0^{DD}(\mathbf{r}^{'},\mathbf{r}^{''},\omega)}{\partial\mathbf{n}^{'}\partial\mathbf{n}^{''}}d\mathbf{s}^{'}, \qquad (3)$$

respectively. In equations (2) and (3), the prediction needs the field on the ms and the source wavelet, $A(\omega)$. G_0^{DD} is the Green's function that vanishes both at the free surface and the ms. In principle, the above formulae are exact. We will see in the numerical test that using these formulae, we get very good deghosting results.

In many cases the source wavelet, $A(\omega)$, is not available. However, for cable depths ~ 6.0m, and wave velocity ~ 1500m/s, and frequencies $f < 125$Hz, G_0^{DD} and its derivative vanish very quickly with increasing offset (T.H. Tan, 1999 and Weglein et al., 2002). So, at large offsets, we can safely ignore the first terms in equations (2) and (3). That is,

$$P(\mathbf{r}^{''}, \mathbf{r}_s, \omega) \approx \int\limits_{ms} P(\mathbf{r}^{'}, \mathbf{r}_s, \omega) \frac{\partial G_0^{DD}(\mathbf{r}^{'}, \mathbf{r}^{''}, \omega)}{\partial \mathbf{n}^{'}} d\mathbf{s}^{'} \tag{4}$$

$$\frac{\partial P(\mathbf{r}^{''}, \mathbf{r}_s, \omega)}{\partial \mathbf{n}^{''}} \approx \int\limits_{ms} P(\mathbf{r}^{'}, \mathbf{r}_s, \omega) \frac{\partial^2 G_0^{DD}(\mathbf{r}^{'}, \mathbf{r}^{''}, \omega)}{\partial \mathbf{n}^{'} \partial \mathbf{n}^{''}} d\mathbf{s}^{'} \tag{5}$$

where $\mathbf{r}^{''}$ is on $\tilde{ms}$ and $\mathbf{r}^{'}$ on actual ms, $\mathbf{r}$ is the deghosted output data point, $\mathbf{r}$ is above $\mathbf{r}^{''}$, and $\mathbf{r}^{''}$ is above $\mathbf{r}^{'}$.

We have found, through analytic and numerical tests, that when $\tilde{ms}$ is close to ms, equation (4) works very well everywhere on the $\tilde{ms}$, including at positions directly under the source. However, equation (5) for the derivative of the field works well only at large offsets. For positions under the source, the first term on the right-hand side of equation (3) dominates and so it can not be ignored. In order to work around this issue, we approximate the source wavelet from the data on the measurement surface so that we can include this dominant term.

Notice that the field in the integral in the above formulae consist of two parts: the direct wave $P_0 = A(\omega) G_0^D$ and the scattered field P_s.

$$\begin{aligned}
&\int\limits_{ms} P(\mathbf{r}^{'}, \mathbf{r}_s, \omega) \frac{\partial G_0^{DD}(\mathbf{r}^{'}, \mathbf{r}^{''}, \omega)}{\partial \mathbf{n}^{'}} d\mathbf{s}^{'} \\
= &\int\limits_{ms} \left[A(\omega) G_0^D(\mathbf{r}^{'}, \mathbf{r}_s, \omega) + P_s(\mathbf{r}^{'}, \mathbf{r}_s, \omega) \right] \frac{\partial G_0^{DD}(\mathbf{r}^{'}, \mathbf{r}^{''}, \omega)}{\partial \mathbf{n}^{'}} d\mathbf{s}^{'} \\
= &\ A(\omega) \int\limits_{ms} G_0^D(\mathbf{r}^{'}, \mathbf{r}_s, \omega) \frac{\partial G_0^{DD}(\mathbf{r}^{'}, \mathbf{r}^{''}, \omega)}{\partial \mathbf{n}^{'}} d\mathbf{s}^{'} \\
+ &\int\limits_{ms} P_s(\mathbf{r}^{'}, \mathbf{r}_s, \omega) \frac{\partial G_0^{DD}(\mathbf{r}^{'}, \mathbf{r}^{''}, \omega)}{\partial \mathbf{n}^{'}} d\mathbf{s}^{'}
\end{aligned} \tag{6}$$

and

$$\int\limits_{ms} P(\mathbf{r}^{'}, \mathbf{r}_s, \omega) \frac{\partial^2 G_0^{DD}(\mathbf{r}^{'}, \mathbf{r}^{''}, \omega)}{\partial \mathbf{n}^{'} \partial \mathbf{n}^{''}} d\mathbf{s}^{'}$$

$$= A(\omega) \int_{ms} G_0^{DD}(\mathbf{r}', \mathbf{r}_s, \omega) \frac{\partial^2 G_0^{DD}(\mathbf{r}', \mathbf{r}'', \omega)}{\partial \mathbf{n}' \partial \mathbf{n}''} d\mathbf{s}' + \int_{ms} P_s(\mathbf{r}', \mathbf{r}_s, \omega) \frac{\partial^2 G_0^{DD}(\mathbf{r}', \mathbf{r}'', \omega)}{\partial \mathbf{n}' \partial \mathbf{n}''} d\mathbf{s}' \qquad (7)$$

In the next section, we show that for positions directly under the source on the $\tilde{ms}$, the effect of P_0 is much larger than that of P_s. In that case, we may assume the effect of P_s is zero. Then, since the left-hand side of equation (6) and (7) are known, we can get two estimates of the wavelet, $A(\omega)$: one from equation (6) and the other from equation (7).

For the case when the source is below the ms, equations (4) and (5) are exact and so knowledge of the wavelet $A(\omega)$ is not required. It may be easier to understand through the derivation of equations (2) and (3).

3 Numerical test

We generate a synthetic data set described in Fig. 1. There are four sources in the model. S1 corresponds to the actual air gun with wavelet $A1(\omega)$. S2, S3 and S4 are passive sources, with wavelet $A2(\omega)$, $A3(\omega)$ and $A4(\omega)$ respectively, synthesized in order to give an up-going field on the ms The free surface is modeled as a perfect reflector. The distance between the ms and the free surface is $b = 6.0$ m. All calculations are performed in the frequency domain and we present results for the single frequency k=0.3 m^{-1} (or $f \sim 74Hz$, for water speed=1500m/s). In all cases, the distance between $\tilde{ms}$ and ms is 0.1m and the deghosted data ouput points are 0.1m above $\tilde{ms}$. In our calculations, we have chosen $A(\omega)$ to be real and equal to 1.0. Therefore, we compare only the real part of the P, $\frac{\partial P}{\partial \mathbf{n}}$ and $P^{\mathrm{deg}\,hosted}$.

The total wave field on M.S and exact up-going field are shown in Fig. 2. Figure 3 is the result of the deghosting algorithm using the wavelet $A1(\omega)$ compared to the exact up-going field. The results are very good.

However, if we don't have the wavelet, we use equations (4) and (5) to approximate the field and its derivative, and then use equation (1) to do deghosting. These results are showed in Fig. 10. Why do we get such poor results? Figures 4 and 5 show the predicted wave field and derivative of the wave field, respectively, when we don't know the wavelet. From these graphs, we see that the problem is the derivative of the wave field near the source. For positions near the source, $A(\omega)\frac{\partial G_0^{DD}(\mathbf{r}'', \mathbf{r}_s, \omega)}{\partial \mathbf{n}''}$ in equation (3) makes a large contribution and so we can't ignore it in our prediction.

In order to get a better derivative of the wave field near the source, we first try to get an approximate wavelet so that we can include $A(\omega)\frac{\partial G_0^{DD}(\mathbf{r}'', \mathbf{r}_s, \omega)}{\partial \mathbf{n}''}$. As has been described, we

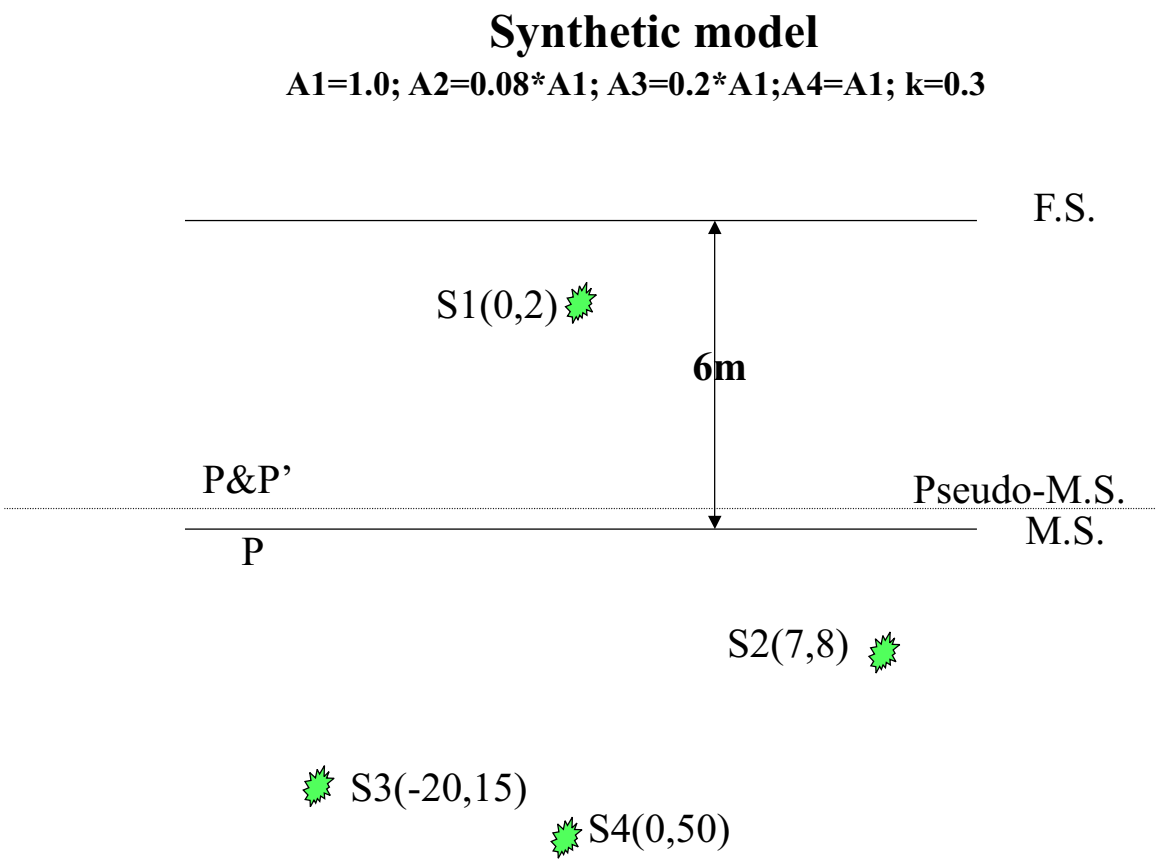

Figure 1: Synthetic model. S1 corresponds to the active source. S2, S3 and S4 are three sources that generate the up-going field. Their (x, z) coordinates are given. All of the calculations are restricted to one frequency k=0.3.

can get an approximation of the wavelet in Fig. 6 and Fig. 7 which show the first term and the sum of the first term and the second term, respectively, in equations (6) and (7). We find that for positions directly under the source, the first term dominates, especially in equation (6). Hence, we can get an approximate value for the wavelet $A = 0.9982$ in Fig. 6 and $A = 1.135$ in Fig. 7., while the exact value is 1.0. Then we add the corresponding first term in equations (2) and (3), respectively, to the predicted value from equations (4) and (5). The new results for the predicted field and its derivative are presented in Fig. 8 and Fig. 9. Using these new results, we do deghosting as before. The results, shown in Fig. 10, are encouraging.

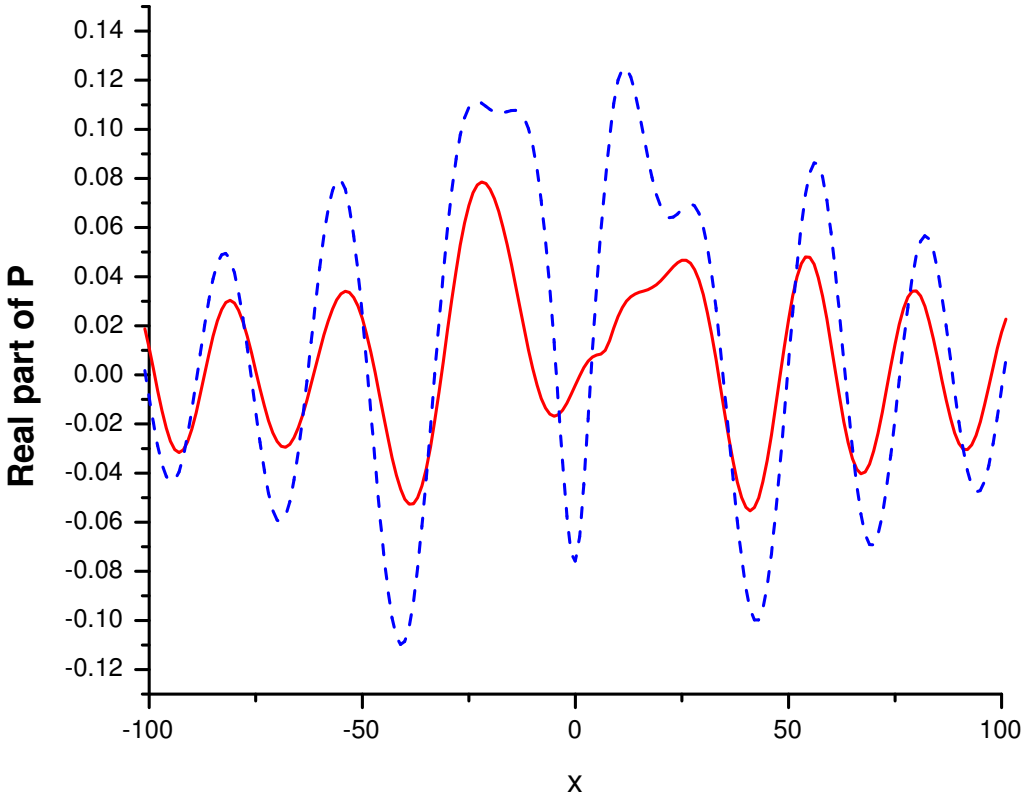

Figure 2: Red solid: Exact total field on ms. Blue dash: Exact up-going field on the surface 0.2m above the ms. x is the source-receiver offset along the ms.

4 Conclusion and discussion

In this paper we have presented some initial tests of the deghosting algorithm given by Weglein et al. (2002). Using the source wavelet, this method works well. For the ocean bottom case, if we have the pressure measurements and the source wavelet, we can use the triangle relationship among pressure, derivative of pressure and the source wavelet to predict the derivative of pressure (Amundsen et al. 1995). We anticipate that this algorithm will be robust (insensitive to depth) and give useful results.

It's important to note that we would like to keep the instrument response factor in the field data and in estimation of the wavelet that derived from other measurements. So, the source wavelet, pressure and the resulted derivative of pressure will have the same factor and the deghosted data will have the same instrument response.

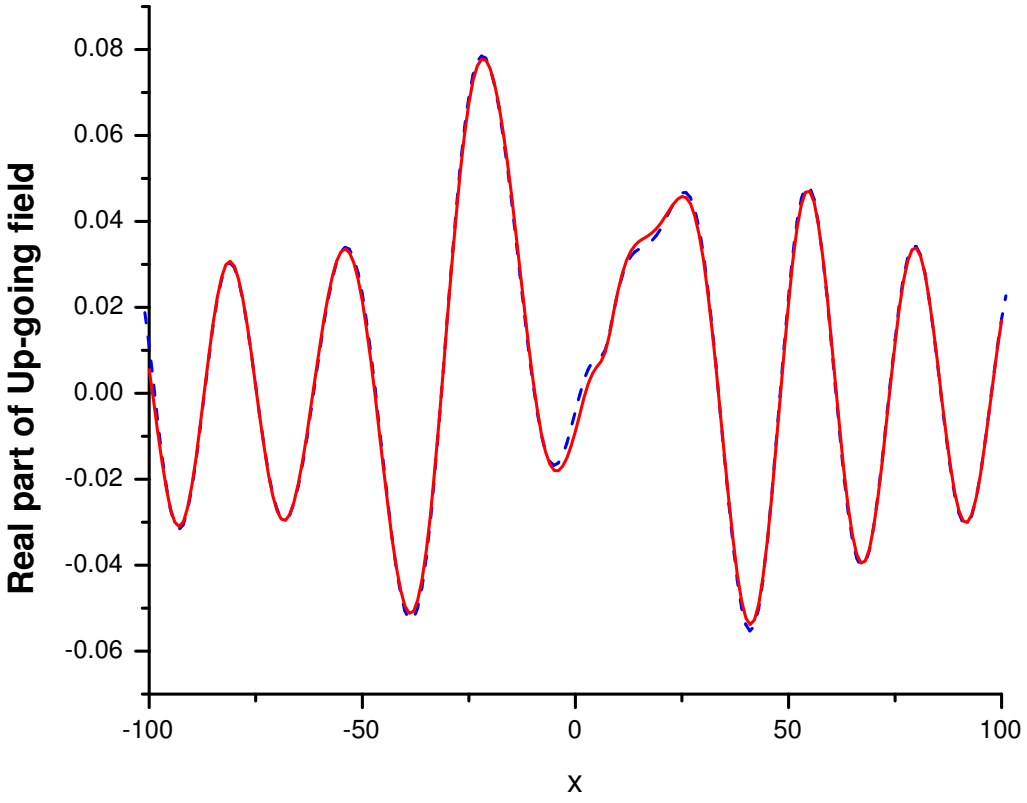

Figure 3: Red solid: Exact up-going field on the surface 0.2m above the ms. Blue dash: Deghosting algorithm results using exact source wavelet. x is the source-receiver offset along the ms.

For towed streamer data if we don't know the wavelet, we provide an approximation method to get the wavelet using only measurements of pressure along the measurement surface. Further tests will be needed before we deal with field data.

Acknowledgements

We thank Simon Shaw, T.H.Tan, Gustavo Correa and Haiyan Zhang for helpful discussions.

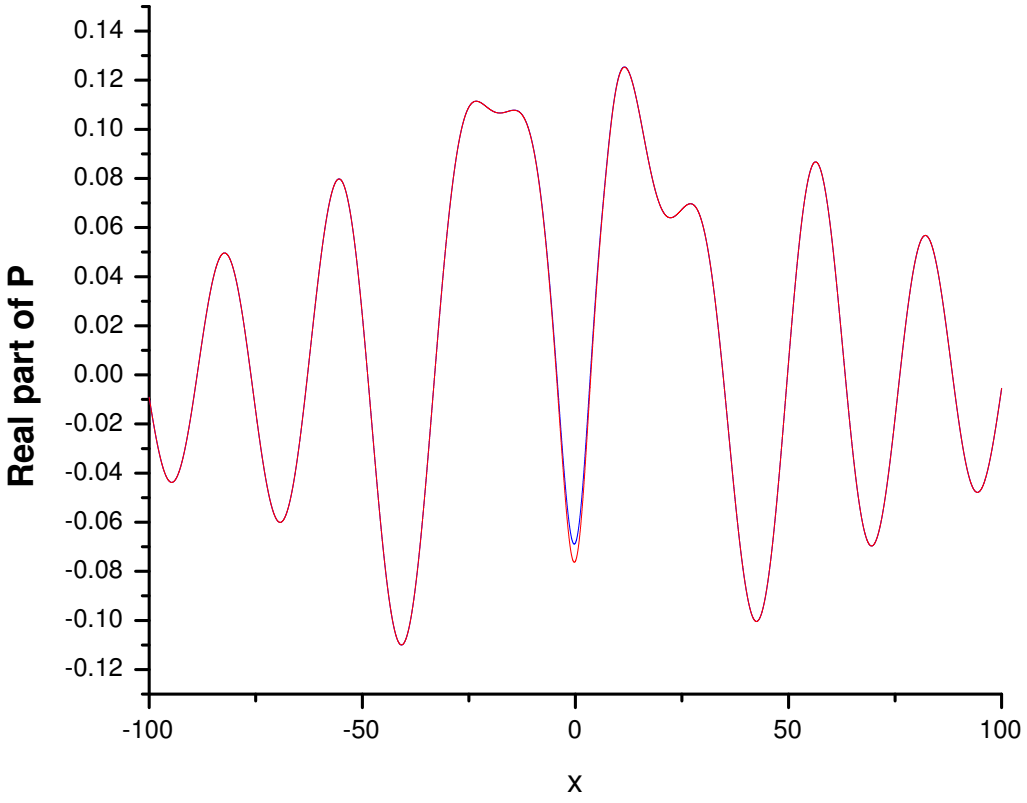

Figure 4: Red solid: Exact field on $\tilde{m}s$. Blue dash: Predicted field on $\tilde{m}s$ without using wavelet.

References

1. Amundsen, L., B.G. Secrest and B. Arntsen, 1995, Extraction of the normal component of the particle velocity from marine pressure data: Geophysics, **60**, 212-222.

2. Osen, A., B.G. Secrest, L.Admundsen and A. Reitan, 1998, Wavelet estimation from marine pressure measurements: Geophysics, **63**, 2108-2119.

3. Tan, T.H., 1992, Source signature estimation: Presented at the Internat. Conf. And Expo. Of Expl. And Development Geophys., Moscow, Russia

4. Tan, T.H., 1999, Wavelet spectrum estimation: Geophysics, **64**, 6, 1836-1846

5. Weglein, A.B., S.A. Shaw, K.H. Matson, J.L. Sheiman, R.H. Stolt, T.H. Tan, A.

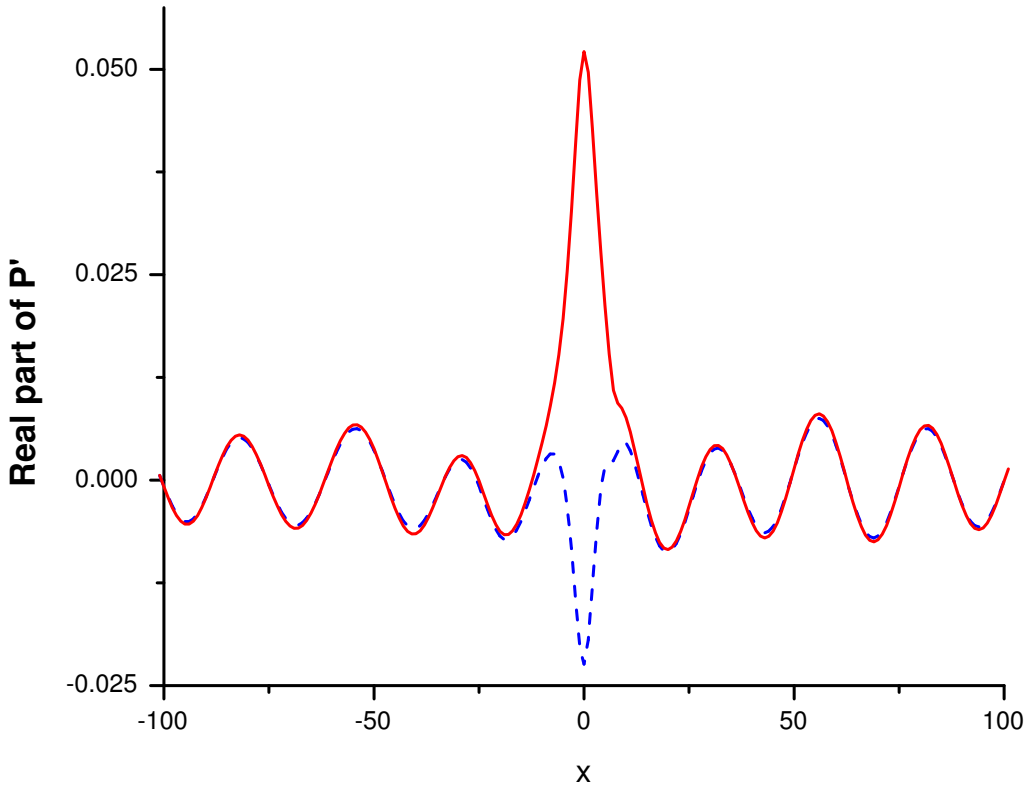

Figure 5: Red solid: Exact derivative of field on $\tilde{m}s$. Blue dash: Predicted derivative of field on $\tilde{m}s$.

Osen, G.P. Correa, K.A. Innanen, Z. Guo and J. Zhang, (2002), New approaches to deghosting towed-streamer and ocean-bottom pressure measurements, 72nd SEG Annual Meeting, Salt Lake City, Utah.

General References

1. Amundsen, L., 1993, Wavenumber-based filtering of marine point source data: Geophysics, **58**, 1335-1348.

2. Ball, V.L. and Corrigan, D., 1996, Dual sensor summation of noisy ocean-bottom data, 66th Ann. Internat. Mtg: Soc. of Expl. Geophys., 28-31.

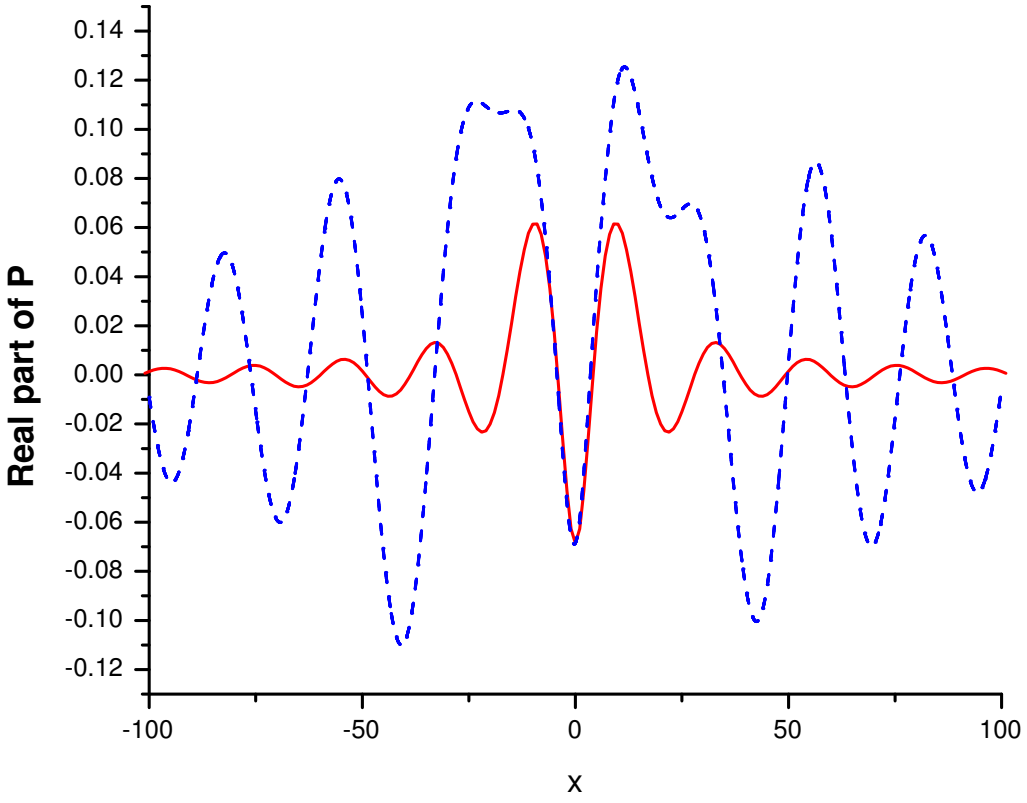

Figure 6: Red solid: The integral value due to the direct wave in Equation (6). Blue dash: The total integral value in Equation (6).

3. Barr, F.F. and Sanders, J.I., 1989, Attenuation of water column reverberations using pressure and velocity detectors in a water-bottom cable, 59th Ann. Internat. Mtg: Soc. of Expl. Geophys., 653-656.

4. Delima, G.R., Weglein, A.B., Porsani, M.J., and Ulrych, T.J., 1990, Robustness of a new source-signature estimation method under realistic data conditions: A deterministic-statistical approach: 60^{th} Ann. Internat. Mtg. SOc. Expl. Geophys. Expanded Abstracts, 1658-1660.

5. Dragoset, B., and Barr, F.J., 1994, Ocean-bottom cable dual-sensor scaling: 64^{th} Ann. Internat. Mtg. SOc. Expl. Geophys. Expanded Abstracts, 857-860.

6. Fokkema, J., and van den Berg, P.M., 1993, Seismic applications of acoustic reciprocity:

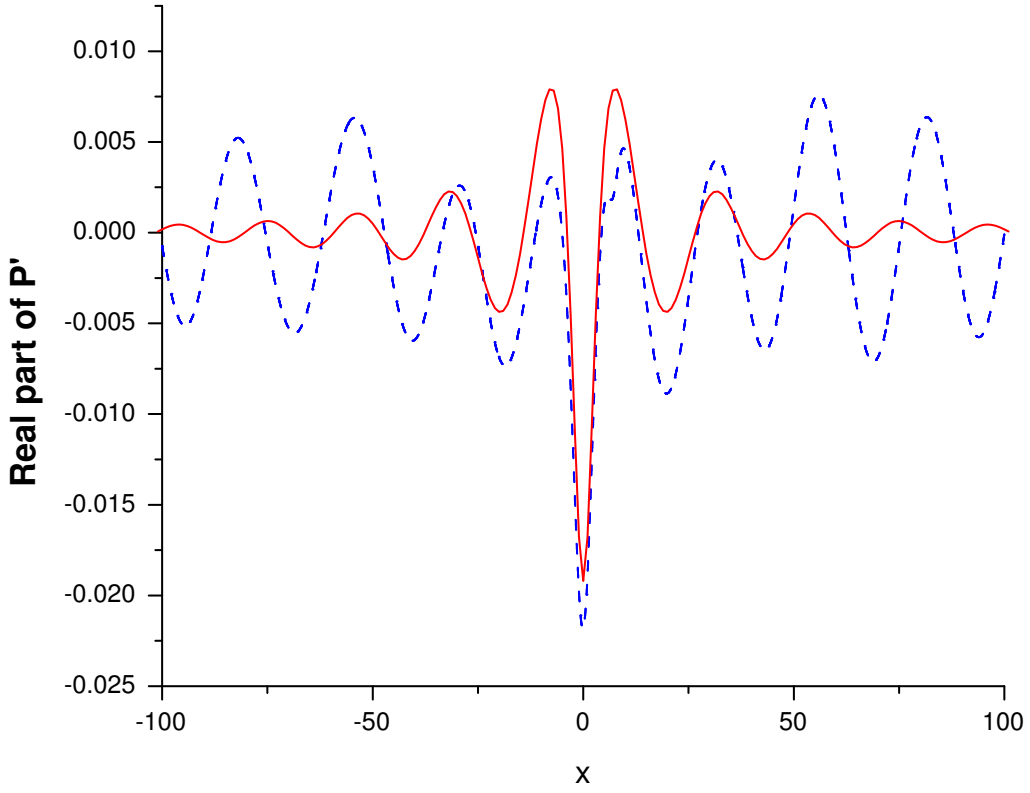

Figure 7: Red solid: The integral value due to the direct wave in Equation (7). Blue dash: The total integral value in Equation (7).

Elsevier Science Publ..

7. Schneinder, W.A., Larner, K.L., Burg, J.P., and Backus, M.M., 1964, A new data processing technique for the elimination of ghost arrivals on reflection seismograms: Geophysics, **29**, 5, p. 783-805

8. Weglein, A.B., Tan, T.H., Shaw, S.A., Matson, K.H., Foster, D.J., 2000, Prediction of the wavefield anywhere above an ordinary towed streamer, 70^{th}Annual Meeting of the Society of Exploration Geophysicists, Calgary, Canada.

9. Ziolkowski, A., 1980, Source array scaling for wavelet deconvolution: Geophysical Prospecting, **28**, 902-918

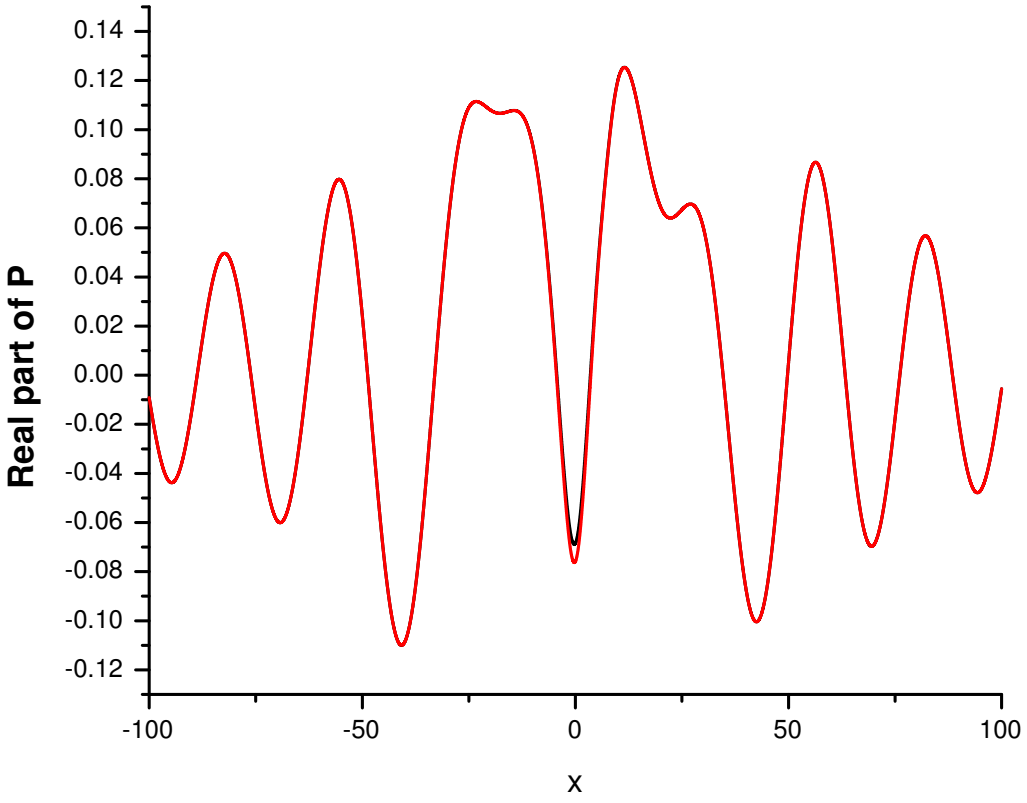

Figure 8: Red solid: Exact field on $\tilde{m}s$. Blue dash: Predicted field on $\tilde{m}s$ using estimated wavelet 0.9982 (covered by red). Black solid: Predicted field on $\tilde{m}s$ without using wavelet.

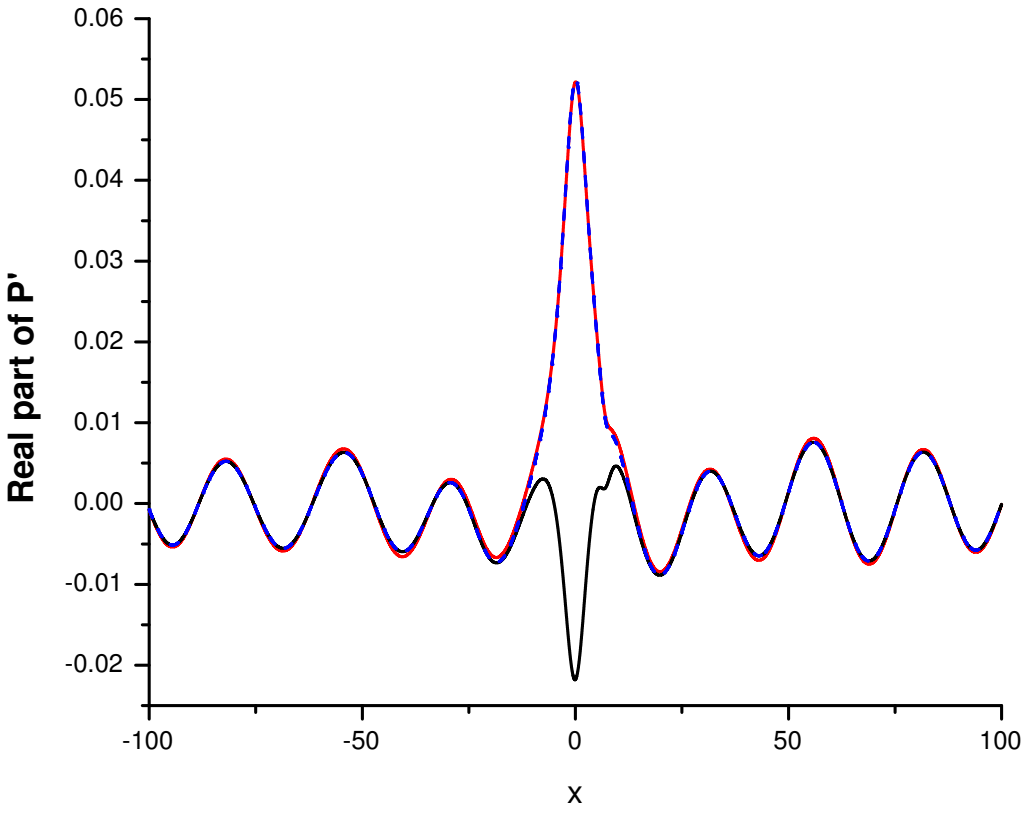

Figure 9: Red solid: Exact derivative of field on $\tilde{m}s$. Blue dash: Predicted derivative of field on $\tilde{m}s$ using estimated wavelet 0.9982 (covered by red). Black solid: Predicted derivative of field on $\tilde{m}s$ without using wavelet.

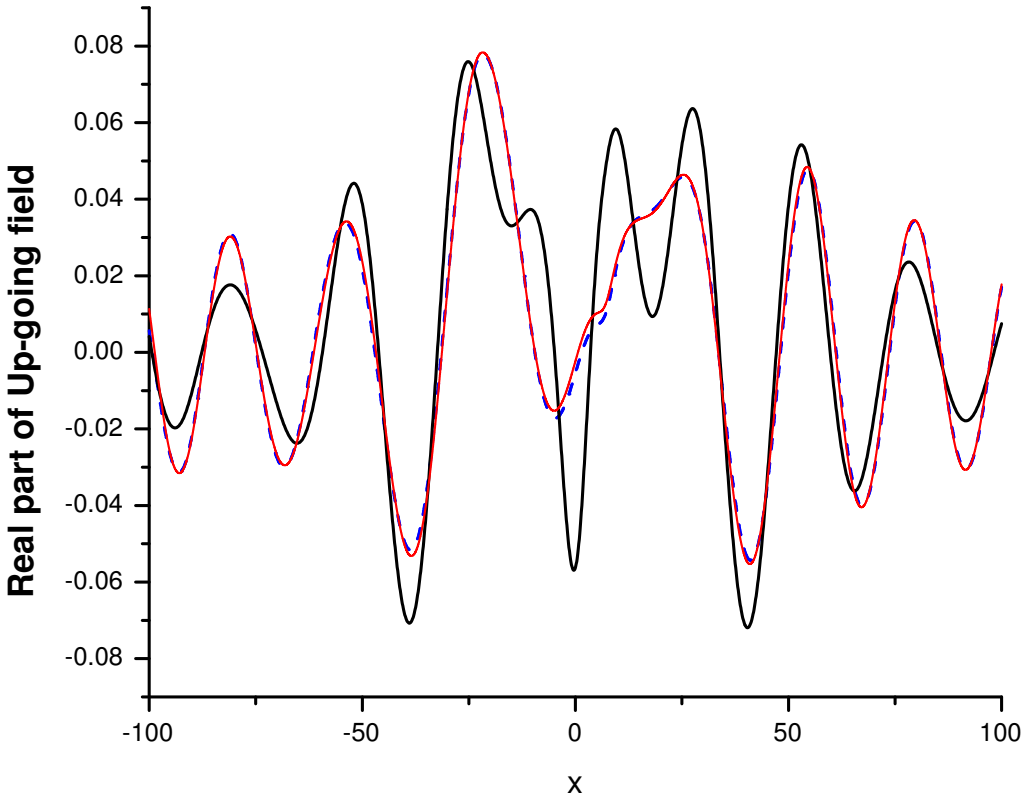

Figure 10: Red solid: Exact up-going field on surface 0.2m above the ms. Blue dash: Deghosting algorithm results using estimated wavelet (0.9982). Black solid: Deghosting algorithm results without using wavelet.